



**EUROfusion**

WPS1-CPR(17) 17596

A Puig Sitjes et al.

# **Wendelstein 7-X Near Real-time Image Diagnostic System for Plasma Facing Components Protection**

Preprint of Paper to be submitted for publication in Proceeding of  
2nd IAEA Technical Meeting on Fusion Data Processing, Validation  
and Analysis



This work has been carried out within the framework of the EUROfusion Consortium and has received funding from the Euratom research and training programme 2014-2018 under grant agreement No 633053. The views and opinions expressed herein do not necessarily reflect those of the European Commission.

This document is intended for publication in the open literature. It is made available on the clear understanding that it may not be further circulated and extracts or references may not be published prior to publication of the original when applicable, or without the consent of the Publications Officer, EUROfusion Programme Management Unit, Culham Science Centre, Abingdon, Oxon, OX14 3DB, UK or e-mail [Publications.Officer@euro-fusion.org](mailto:Publications.Officer@euro-fusion.org)

Enquiries about Copyright and reproduction should be addressed to the Publications Officer, EUROfusion Programme Management Unit, Culham Science Centre, Abingdon, Oxon, OX14 3DB, UK or e-mail [Publications.Officer@euro-fusion.org](mailto:Publications.Officer@euro-fusion.org)

The contents of this preprint and all other EUROfusion Preprints, Reports and Conference Papers are available to view online free at <http://www.euro-fusionscipub.org>. This site has full search facilities and e-mail alert options. In the JET specific papers the diagrams contained within the PDFs on this site are hyperlinked

# Wendelstein 7-X Near Real-time Image Diagnostic System for Plasma Facing Components Protection

A. Puig Sitjes<sup>1</sup>, M. Jakubowski<sup>1</sup>, A. Ali<sup>1</sup>, P. Drewelow<sup>1</sup>, F. Pisano<sup>2</sup>, V. Moncada<sup>3</sup>, T.T. Ngo<sup>4</sup>, B. Cannas<sup>2</sup>, J.M. Travere<sup>4</sup>, G. Kocsis<sup>5</sup>, T. Szepesi<sup>5</sup> and W7-X Team<sup>1</sup>

<sup>1</sup> Max-Planck-Institut für Plasmaphysik, Wendelsteinstraße 1, 17491 Greifswald, Germany.

<sup>2</sup> University of Cagliari, Piazza d'Armi, 09126 Cagliari, Italy.

<sup>3</sup> ThemaDIAG, 100 Impasse des Houllieres, ZA Le Pontet, F-13590 Meyreuil, France.

<sup>4</sup> CEA, IRFM, F-13108 Saint Paul-lez-Durance, France.

<sup>5</sup> Wigner RCP, RMI, Konkoly Thege 29-33, H-1121 Budapest, Hungary.

E-mail: aleix.puig.sitjes@ipp.mpg.de

June 2017

## Abstract.

Wendelstein 7-X (W7-X) fusion experiment is aimed at proving that the stellarator concept is suitable for a future fusion reactor. Therefore, it is designed for steady-state plasmas of up to 30 minutes, which means that the thermal control of the Plasma Facing Components (PFCs) is of vital importance to prevent damages to the device.

In this paper an overview of the design of the Near Real-time Image Diagnostic System for PFCs protection in W7-X is presented. The goal of the System is to monitor the PFCs with high risk of permanent damage due to local overheating during plasma operations and send alarms to the Interlock System. The monitoring of the PFCs is based on thermographic and video cameras and their video streams are analyzed by means of GPU-based computer vision techniques to detect the strike-line, hot spots and other thermal events. The video streams and the detected thermal events are displayed on-line in the control room in the form of a thermal map and permanently stored in the database. In order to determine the emissivity and maximum temperature allowed, a pixel-based correspondence between the image and the observed device part is required. The 3D geometry of W7-X makes the System particularly sensitive to the spatial calibration of the cameras since hot spots can be expected anywhere and a full segmentation of the field of view is necessary, in contrast to other ROI-based systems. A precise registration of the field of view and a correction of the strong lens distortion caused by the wide-angle optical system are then required.

During the next operation phase the uncooled graphite divertor units will allow to test the System without risk of damaging the divertors in preparation when water-cooled high-heat flux divertors will be used.

*Keywords:* W7-X, imaging diagnostics, plasma facing components

## I. Introduction

Wendelstein 7-X (W7-X) is a drift optimized nuclear fusion device of stellarator type build in Greifswald by the Max-Planck-Institut für Plasmaphysik (IPP).<sup>1</sup> Its main goal is to prove that the stellarator design is suitable for a future fusion power plant with steady-state operation. With plasmas of up to 30 minutes and with a steady-state heating power of 10 MW a continuous real-time data acquisition, analysis and control system is necessary in order to protect the Plasma Facing Components (PFCs) from overheating.

The road-map to steady-state operation consists of different Operating Phases (OP) with increasing machine performance with every phase. The so-called OP1.2 test phase, planned for the second half of 2017 and the first half of 2018, will be used to test the Near Real-time Image Diagnostic System aimed to protect the PFCs during the steady-state operation. During this phase, an inertially cooled graphite divertor will be used, and the system will be tested without risk of damaging the divertor. After this phase, further developments will follow in order to port the near real-time system (on-line, but not real-time) to a true real-time operating system with deterministic behavior.<sup>2</sup> In OP2, planned for the beginning of 2020, a high heat flux (HHF) water-cooled divertor will be installed and the system shall be able to protect the PFCs in steady state operation.

This paper is organized as follows. Section II describes the PFCs operational limits and the main requirements of the system. In Section III an overview of the imaging system and the technical specifications of the endoscopes, immersion tubes and the thermographic and video cameras are given. In Section IV, the software architecture and main functions are introduced. Section V describes the image processing algorithms used to detect and classify the hot spots and to detect and analyze the strike-line shapes. And Section VI describes the structure of the detected thermal events and how the generated metadata is displayed in the control room. Finally, in Section VII the conclusions and the future work outlook are given.

## II. Plasma facing components operational limits

W7-X is a 3D helically shaped stellarator with 5 symmetric modules and 10 divertors (5 upper and 5 lower divertor units) utilizing large magnetic islands for heat and particle exhaust. In OP2, the high heat flux water-cooled target elements will be made of Carbon Fiber Composite (CFC) tiles which are joined to a CuCrZr heat sink (see Figure 1). The thickness of the tile depends on its position in the divertor due to the 3D shape of the device (up to a maximum value of 2 mm). The divertors have three target elements: the vertical target, the low-iota and high-iota horizontal targets. Between the low-iota and high-iota horizontal targets there is a low-loaded central part made of graphite tiles. The other water-cooled PFCs are the baffles, the heat shields and the wall and pumping gap panels. The baffles and the heat shields are made of graphite tiles bolted on CuCrZr and the wall and pumping gap panels are made of stainless steel.<sup>3</sup>

PFC	Material	Max. heat flux	Max. temp.
OP1.2 Test divertor targets	Graphite	10 MW/m <sup>2</sup>	1600 °C
OP2 HHF divertor targets	CFC	10 MW/m <sup>2</sup>	1000 °C
Divertor central part	Graphite	1 MW/m <sup>2</sup>	1000 °C
Baffles	Graphite	0.5 MW/m <sup>2</sup>	1000 °C
Heat shields	Graphite	350 KW/m <sup>2</sup>	1000 °C
Wall panels	Stainless steel	100 KW/m <sup>2</sup>	150 °C
Pumping gap panels	Stainless steel	100 KW/m <sup>2</sup>	150 °C

**Table I.** The Plasma Facing Components (PFCs) operational limits.

W7-X has a total steady-state plasma heating power of 10 MW provided by the Electron Cyclotron Resonance Heating (ECRH), which can operate up to 30 minutes. Together with the main heating source, two more systems provide additional power for a short period of time (up to 10s): the Neutral Beam Injection (NBI), which provides 10 MW, and the Ion Cyclotron Resonance Heating (ICRH), which provides 4 MW. The divertor target elements are designed to dissipate up to 10 MW/m<sup>2</sup> in continuous operation. The graphite element between the high-iota and low-iota divertor targets can dissipate up to 1 MW/m<sup>2</sup>. The baffles can dissipate 0.5 MW/m<sup>2</sup>, the heat shields 350 kW/m<sup>2</sup> and the wall and pumping gap panels 100 kW/m<sup>2</sup>. Table I summarizes the operational limits of the PFCs.

The consequences of overloading the divertor target elements are the increase of thermal resistance and, thus, a reduced performance of the element, and at the end the delamination of the tile. This can lead to a complete de-bonding and loss of the thermal connectivity to the cooling structure of the tile. The Cu interlayer of the divertor tiles cannot exceed a temperature of 475 °C to prevent these damages. If the surface temperature reaches 1200 °C, the Cu interlayer reaches the maximum temperature in 3 s. For safety, the system will send an alarm to the Interlock System when the surface reaches 1000 °C and the plasma control system is required to react and change the scenario within 1 s. This means that the system must detect a hot spot, analyze its risk and send an alarm within 100-200 ms.

### III. The imaging system

The imaging system consists of 10 infrared cameras and 10 video cameras. In OP1.2, 9 immersion tubes and 1 endoscope<sup>4-6</sup> will be tested to observe the 10 divertors in the infrared range. The mixture of the diagnostic is a result of different requirements for different PFCs and historical development of W7-X. It is also not a final set-up of the diagnostics. In OP2, with full heating power of 10 MW for 30 minutes, the uncooled immersion tubes cannot survive the radiation from the plasma. Therefore, they will be replaced by water-cooled endoscopes. The video system, covering the visible spectrum, is based on the Event Detection Intelligent Cameras (EDICAM) systems<sup>7-10</sup> providing

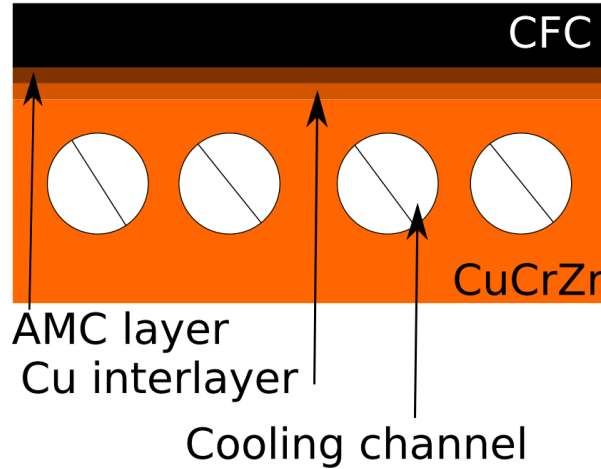


**Figure 1.** The divertor tile structure is made of a Carbon Fiber Composite (CFC) layer joined to a AMC layer and a Cu layer. The bi-layer tiles are then joined to a Copper Chromium Zirconium (CuCrZr) cooling structure by electron beam welding. If the surface temperature reaches 1200 °C the Cu interlayer reaches its maximum temperature of 475 °C in 3s (figure adopted from<sup>15</sup>).

a tangential view of the plasma vessel and extra coverage of the walls in order to detect fast particle losses due to the NBI heating. Below we present a short description of the diagnostics. More details can be found in the references.

### *III.A. The immersion tubes*

The immersion tubes provide a field of view of 116° horizontally and 100° vertically with an optical resolution of the order of 5 to 20 mm, depending on the distance and the viewing angle of the divertor. They are equipped with microbolometer cameras IRCam Caleo 678k L covering the spectral range from 8 to 14  $\mu\text{m}$ . They have a sensor size of 1024 x 768 pixels, with a pixel size of 17 x 17  $\mu\text{m}$ , a bit depth of 14 bits and a maximum frame rate of 120 Hz.

### *III.B. The endoscopes*

The prototype of endoscope, designed to monitor the divertors during high heat flux steady-state operation, will be tested in the coming experimental phase. It consists of an off-axis Cassegrain optical system with a pinhole aperture of 6 mm. The light is transmitted to the cameras sensor through two mirrors in the front and the off-axis Cassegrain mirrors. The off-axis design avoids the diffraction caused by the central obstruction. The light is divided by a dichroic splitter into visible and infrared beams, which are detected by the cameras after being corrected by a group of lenses.

The endoscopes monitor the 5 m long and 1 m wide divertors with a field of view of 115° horizontally (-75°, +40°) and 60° vertically (-40°, +20°). The target elements require a resolution of 8 mm in the divertor plane in order to resolve each of the small

tiles forming the divertor. The endoscopes have an optical resolution from 6 mm (at 40% MTF) to 20 mm depending on the distance and the viewing angle of the observed part of the divertor. Therefore the end system needs to significantly improve the optical resolution.

The main part of the endoscope is the infrared camera Infratec ImageIR 9300. These cameras have an Indium Antimonide (InSb) sensor covering the spectral range from 2 to 5.7  $\mu\text{m}$ , with 1280 x 1024 pixels, a pixel size of 15 x 15  $\mu\text{m}$ , a bit depth of 14-bit and a maximum frame rate of 106 Hz.

### *III.C. Event Detection Intelligent Cameras (EDICAMs)*

To protect the walls from localized losses of energetic particles, the intelligent fast video cameras EDICAMs are used. These cameras provide a tangential view of the plasma vessel with a field of view of 30° horizontally and 24° vertically with an optical resolution of 2 mm/pixel. These cameras observe a mixture of PFCs, e.g. stainless-steel wall panels, graphite heat shields, etc.

The EDICAMs cover the visible spectrum from 450 nm to 720 nm, using a CMOS LUPA-1300 sensor with 1280 x 1024 pixels and a pixel size of 14 x 14  $\mu\text{m}$ , a bit depth of 12 bits and a maximum frame rate of 440 Hz. The sensor allows non-destructive read out of the data and the cameras are equipped with an on-board FPGA, which is used to detect thermal events and send trigger alarms in real time to the interlock system. The cameras can analyze multiple, dynamic and arbitrary shaped regions of interest.

## **IV. The software**

### *IV.A. Software functions*

The software is divided into two main applications, which communicate through the network in a server-client topology (see Figure 2). 10 workstations acquire and analyze the video streams from the thermographic cameras and 10 workstations acquire and analyze the images from the EDICAMs. The video streams are stored locally and sent in real time to the control room for visualization. The video streams are analyzed on-line by means of computer vision techniques to detect the strike-line, hot spots and other thermal events. If a critical condition is reached an alarm is sent to the Interlock System and proper action has to be taken: strike-line sweeping, reducing the heating power or stopping the entire experiment. The metadata generated by the image analysis and the triggered alarms are sent to the control room for visualization and saved in a SQL database. The video streams are sent to the permanent archive system after the discharge.

In the control room an application displays the video streams in a 9 x 9 cell grid down-sampled to a resolution of 640 x 480 and 25 Hz, except one video stream upon request which is displayed at full spatial resolution. All the associated metadata, which includes the detected hot spots, strike-lines and generated alarms are also displayed

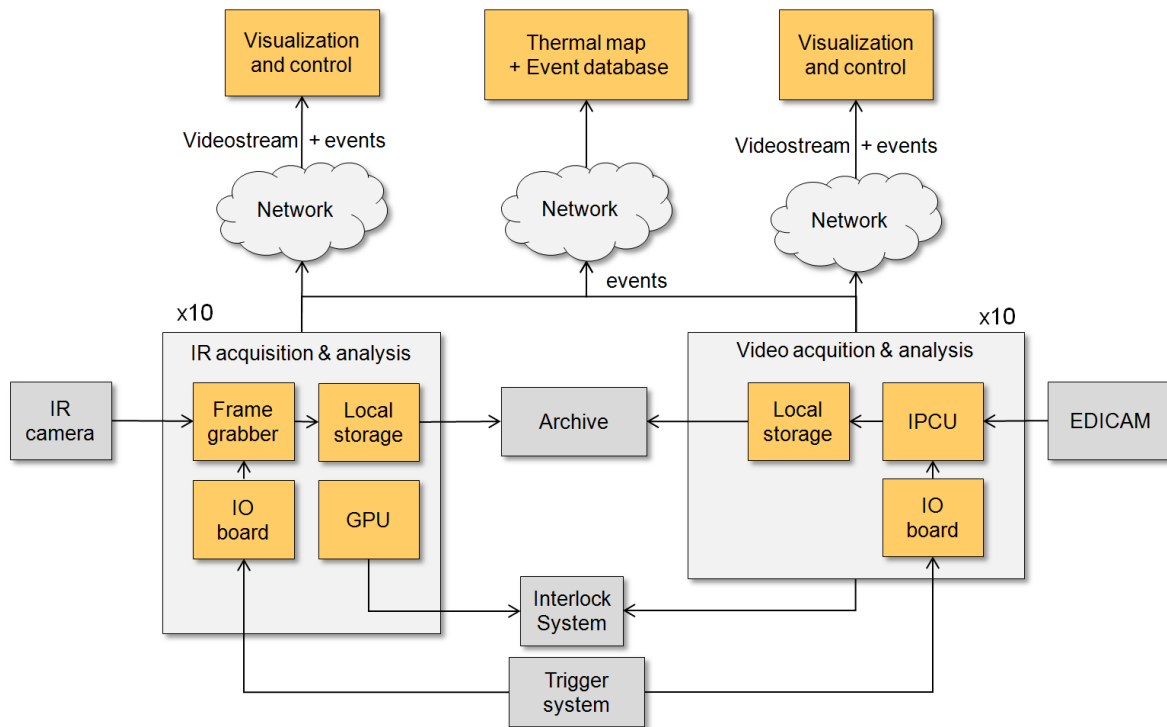


**Figure 2.** The system overview. 10 workstations acquire and analyze the images from the thermographic cameras and 10 workstations acquire and analyze images from 10 EDICAM video cameras. The acquisition workstations analyze the video streams and send alarms to the Fast Interlock System. The video streams and the detected events are also sent to a centralized computer in the control room for visualization and control of the cameras.

overlaid on the video streams. The history and evolution of these events are also shown in a thermal map, which provides an overview of all the thermal events occurring in the entire device.

The software also provides off-line tools to replay the video streams with the detected thermal events just after the discharge.

#### IV.B. Software architecture

The software is based on ThermaVIP SDK,<sup>11,12</sup> a plugin-based open source C++ framework initially developed at CEA designed to process and display multi-modal data for on-line and off-line analysis (see Figure 3). The framework is being further developed by the ThermaDIAG company in collaboration with CEA and IPP and it is aimed to be an open source framework for camera control and image analysis for the fusion community.

The software of the system consists in a set of plugins sitting on top of ThermaVIP SDK for acquisition, trigger management, processing, storage and graphical user interfacing (see Figure 4). ThermaVIP provides tools to create multi-threaded processing pipelines which can take advantage of the multi-core CPU architectures (see



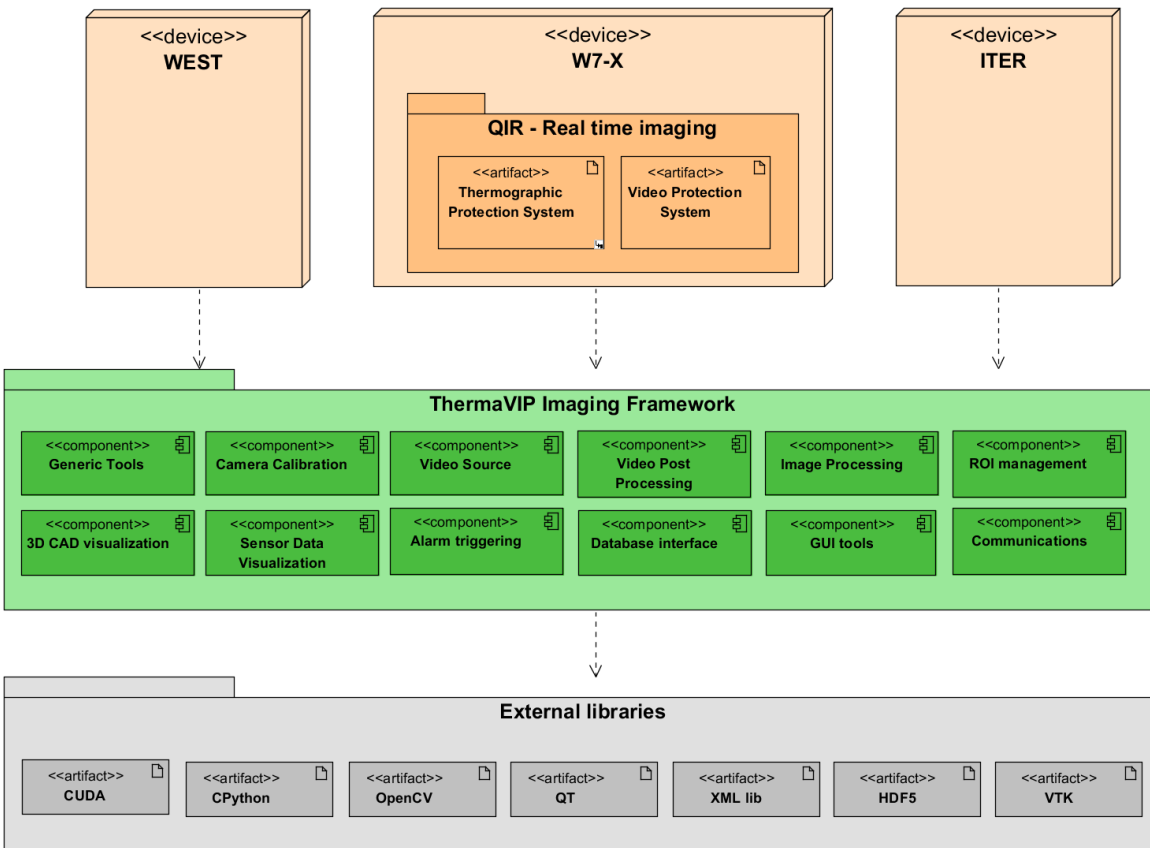


**Figure 3.** ThermaVIP imaging framework. It provides modules for camera control, video processing, ROI management, 3D visualization, alarm triggering, database management, communication and graphical user interface tools.

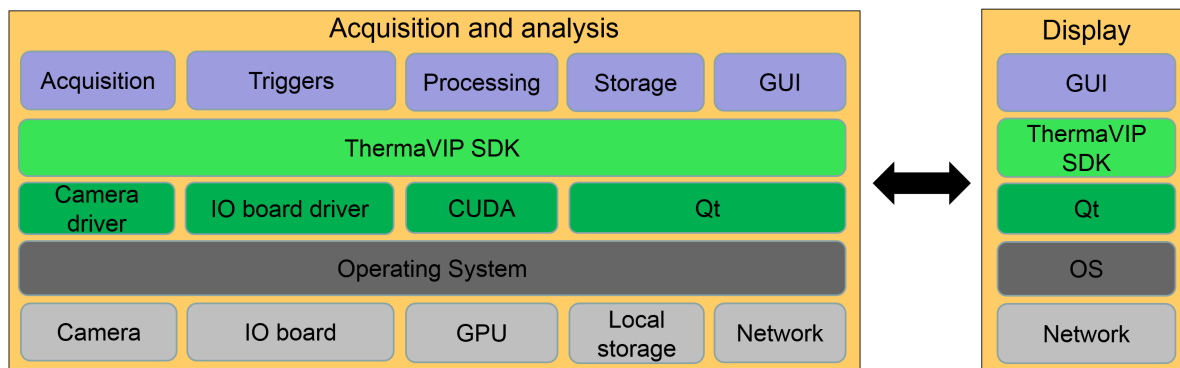


**Figure 4.** The software stack. The software consists in a set of plugins on top of ThermaVIP SDK. It is based on the Qt library which provides portability to different operating systems.

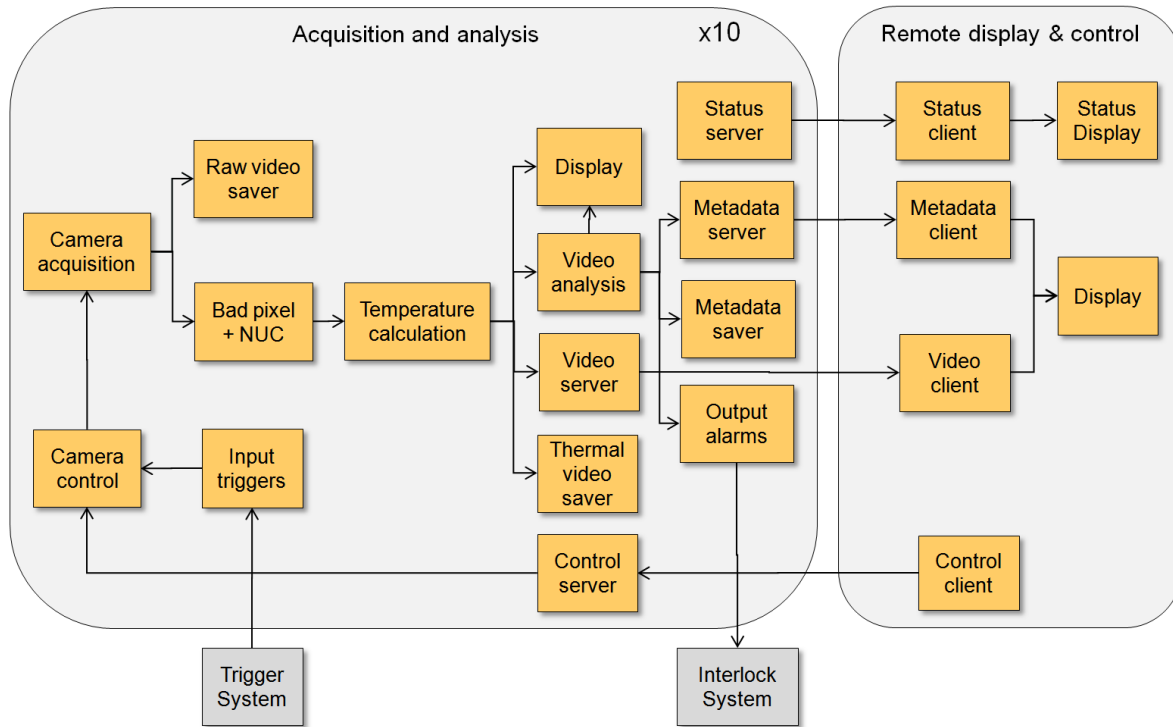


**Figure 5.** The software processing pipeline consists in a set of interconnected processes, each one running in an independent thread, with circular buffers in each connection. 10 acquisition and analysis workstations act as servers and provide the video streams, the metadata and the status information to the remote client, a central workstation that displays the data in the control room.

Figure 5 for a detailed view of the processing pipeline).

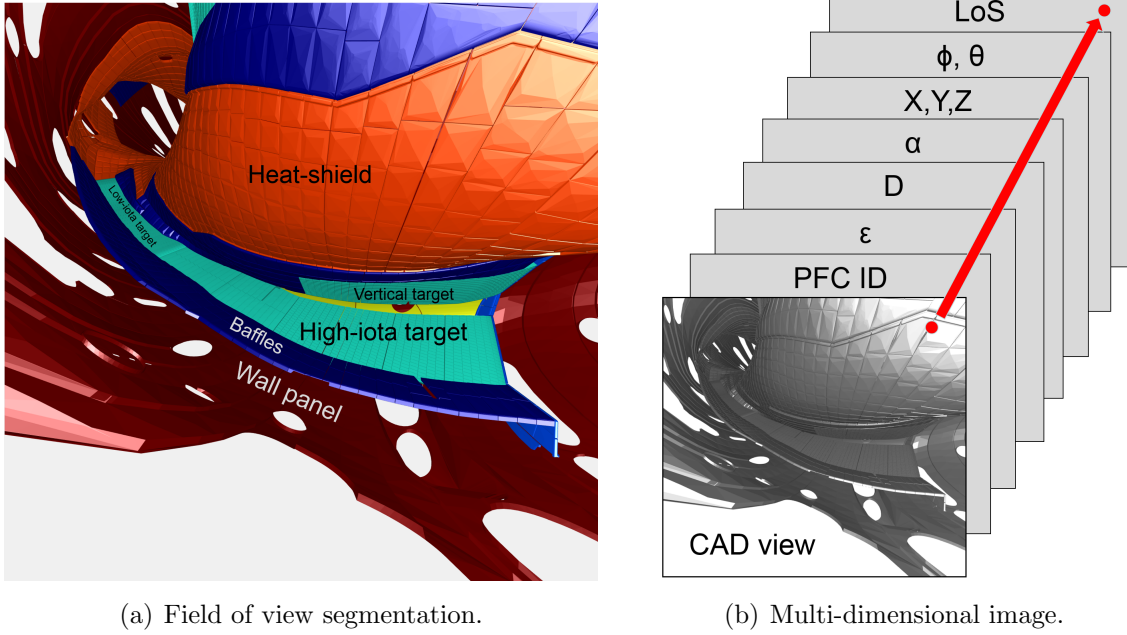
## V. Image analysis

The image analysis consists in the detection and classification of hot spots and the detection and analysis of the strike-line shape in real time. Their temperature and position in the device are evaluated and thermal events and alarms are generated in order to protect the device integrity when a critical event occurs.

The image analysis algorithms have been implemented in a GPU architecture using the CUDA library. They can run in real time, with a processing time of 20 ms per frame, and they have been tested in the GLADIS experiment.<sup>13</sup>

### V.A. Scene model

In order to evaluate the risk of a given thermal event a scene model is required to know its position, physical size and temperature. Because of the 3D geometry of W7-X thermal events can be expected anywhere in the field of view of the cameras. Instead of using a ROI-based scene model, the system uses a full segmentation of the field of view, so that for each pixel there is a correspondence with the CAD model (see Figure 6).



(a) Field of view segmentation.

(b) Multi-dimensional image.

**Figure 6.** The scene model is a full segmentation of the field of view and it stores for each pixel the corresponding PFC, emissivity  $\epsilon$ , distance  $D$  to the target object, the angle  $\alpha$  of the line of sight respect the normal to the surface, the Cartesian world coordinates  $X, Y, Z$ , the polar world coordinates  $\phi, \theta$  and the Line of Sight (LoS). It is saved in a multi-dimensional image for each camera.

This requires a precise geometric calibration of the cameras which has been performed using the Zhang calibration method<sup>14</sup> to compute the intrinsic camera parameters and the lens distortion model. In this case a radial distortion model has been used.

The scene model stores the information of the target elements in a multi-dimensional image in HDF5 format with the following data:

- Emissivity  $\epsilon$  of the target material.
- The distance  $D$  to the target object.
- Angle  $\alpha$  of the line of sight respect the normal to the target surface.
- 3D world Cartesian coordinates of the target point:  $X, Y, Z$ .
- 3D world toroidal and poloidal coordinates of the target point:  $\phi, \theta$ .
- The pixel line of sight.

This information is then used to compute the surface temperature of the thermal event taking into account the emissivity of the material, its distance to the camera and the angle with the normal to the surface. The world coordinates are then used to measure the physical size and the position of the event inside the device. All this information is then stored in a metadata structure.

### *V.B. Hot spot detection*

The system detects the hot spots in the thermographic images by temperature thresholding. The segmented pixels are clustered with a connected components algorithm and they are tracked over time. The scene model provides the information required to evaluate the risk of the hot spot: its position, size, mean and maximum temperature (see Figure 7).

The video streams in the visible spectrum are also analyzed in order to detect "bright spots" due to localized fast particle losses from the neutral beam injection (NBI). In this case, however, only brightness is taken into account and no temperature measurement can be evaluated.

### *V.C. Hot spot classification*

High surface temperatures can be caused by different phenomena:

- A hot spot may show up due to a power overload, in which case the system must react, or otherwise the PFC may suffer serious damages.
- Hot spots may also be caused by fast particle losses from the NBI heating.
- Dust particles can be redeposited and since they are poorly thermally connected with the underlying material they become very hot. They are also a cause of false alarms.
- Due to carbon erosion, thin surface layers can develop on the plasma facing components due to re-deposition. They show as high temperature hot spots due to their low thermal capacity and their poor thermal connectivity to the underlying material and the cooling system. They do not suppose a risk to the PFCs integrity and may be a source of false alarms.
- The delamination of a tile decreases the thermal connectivity of the CFC with the cooling system and the tile can get very hot. This will in turn further damage the tile and at the end it may fail completely. Due to the extreme difficulties of replacing the damaged elements, delaminations have to be detected in time to avoid the complete failure of the tile.

A method has been developed to distinguish the cause of a hot spot by modulating a power source with a train of pulses in order to measure the time evolution of the surface temperature. Due to their different thermal capacity and conductivity the different types of hot spots respond differently. The normalized temperature decay time  $\tau$  defined in equation 1 is a discriminative feature that it is used to classify the origin of a hot spot with an heuristic classification tree.<sup>15</sup>

$$\tau(t) = \frac{T(t)}{\frac{dT}{dt}} \quad (1)$$

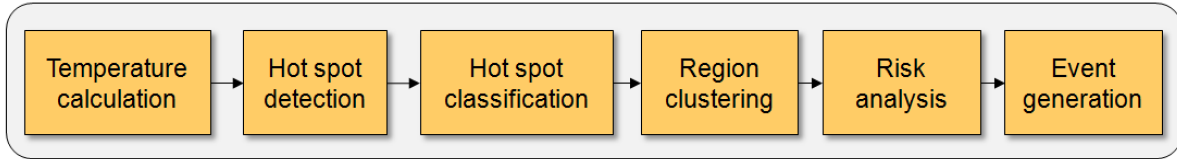


**Figure 7.** The hot spot detection and classification process. The pixels are thresholded and a pixel classification is performed according to the  $\tau$  parameter. Then a region is formed by pixel clustering using a connected components algorithm and the risk of the hot spot is evaluated taking into account the scene model. Finally an event is generated.

### *V.D. Strike-line analysis*

The strike-line is detected and segmented by heat-flux  $\phi$  thresholding:

$$\phi_{th} = \phi_{max} \exp(-1) \quad (2)$$

The strike-line is then projected onto the CAD model using the geometrical calibration of the cameras. After the projection, its position, width, length, mean and maximum heat-flux are evaluated and the corresponding metadata is generated. The mapped image is converted into polar coordinates and its shape is characterized with 2D Fourier descriptors. These features are saved into the database for posterior analysis.

## **VI. Thermal events**

When the image analysis detects a thermal event, it generates a metadata structure which is stored in JSON format (see Figure 8). A thermal event is identified by a unique ID and a timestamp. It can be classified as: hot spot, surface layer, delamination, UFO, reflection, strike-line or bright spot. It can have parent events and child events. These two fields are used, for instance, to track a hot spot that splits or merges. A thermal event is associated with several event views, which is an instance of an event for a given frame. In general a thermal event spans along different frames and it may show different features in each frame. An event view is described by its unique ID, its timestamp, its position in world and image coordinates, its bounding box, its pixel and physical size, and its maximum and mean temperature (or brightness). Each event view is assigned a "criticality" value, depending on its position, size and temperature. The same thermal event can be observed by one or more cameras from different diagnostics.

The system is connected to the Interlock System and a TTL alarm is generated when a thermal event reaches a dangerous condition. The Interlock System notifies the central Safety System (cSS) which is then responsible of taking the proper action to protect the integrity of the device.

The thermal events are stored in a SQL database which is updated in real time. The database can be queried off-line to replay a given thermal event with its corresponding video stream.

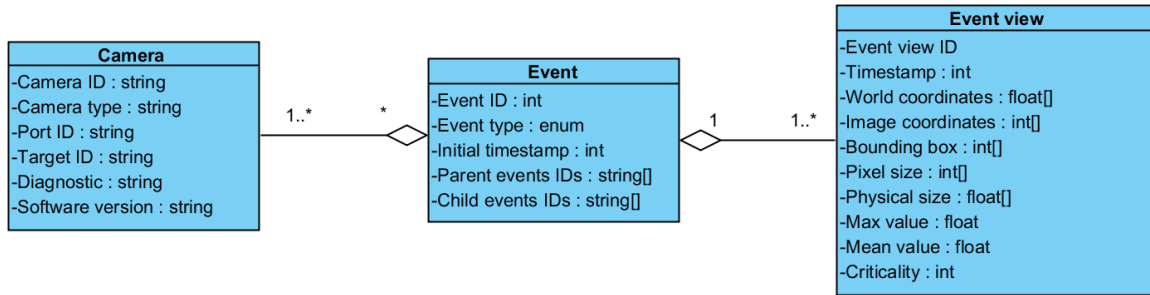


**Figure 8.** The thermal events metadata structure. A thermal event consists of a unique ID and a timestamp. An event can be observed by one or more cameras from different diagnostics and each event can have one or more event views, one for each frame in which is observable.

### VI.A. Thermal map

The thermal map is a 2D representation of the plasma facing components. It is generated by unfolding the 3D helical shape of the device into a 2D surface. The generated metadata is mapped in real time onto the thermal map providing a centralized overview of all the thermal events occurring in the device during the discharge in the control room.

## VII. Conclusions

In this work, the near real time image diagnostic system for the plasma facing components protection of Wendelstein 7-X has been presented. The system will be responsible for the protection of the water-cooled PFCs and, in particular, the high heat flux divertor that will be installed by 2020. This prototype version, however, will be tested during the next operation phase OP1.2 with an inertially cooled divertor in order to validate the overall design and the image processing algorithms. In the following years the work will focus on porting the system to a real time operating system and integrating it into the safety control system of W7-X.

Further work will have to follow to develop a decision-making algorithm that given the thermographic analysis of the PFCs takes, in real time, the optimal decision to protect the device and, in a later stage, optimize the operational performance of the experiment in steady-state operation.

## Acknowledgments

This work has been carried out within the framework of the EUROfusion Consortium and has received funding from the Euratom research and training programme 2014-2018 under grant agreement No. 633053. The views and opinions expressed herein do not necessarily reflect those of the European Commission.

## References

- [1] H.S. BOSCH, V. ERCKMANN et al., "Construction of Wendelstein 7-X Engineering a Steady State Stellarator", *IEEE Transactions on Plasma Science*, **38**, 265-273 (2010).
- [2] H. LAQUA, H. NIEDERMEYER et al., "Real-time Software for the Fusion Experiment WENDELSTEIN 7-X", *Fusion Engineering and Design*, **81**, 1807 (2006).
- [3] J. BOSCARY, R. STADLER et al., "Design and Technological Solutions for the Plasma Facing Components of Wendelstein 7-X", *Fusion Engineering and Design*, **86**, 572-575 (2011).
- [4] R. KÖNIG, J. baldzuhn et al., "Diagnostics Development for Quasi-steady-state Operation of the Wendelstein 7-X Stellarator", *Review of Scientific Instruments*, **83**, 10, 10D730 (2012).
- [5] M. JAKUBOWSKI, C. BIEDERMANN et al., "Development of Infrared and Visible Endoscope as the Safety Diagnostic for Steadystate Operation of Wendelstein 7-X", presented at Quantitative InfraRed Thermography, Bordeaux, France, July 07-11, 2014.
- [6] D. CHAUVIN, M. JAKUBOWSKI et al., "Design and Manufacturing Progress of IRVIS Endoscopes Prototypes for W7-X Divertor Temperature Monitoring", Proceedings of 29th Symposium on Fusion Technology, Prague, Czech Republic, September 5-9, 2016.
- [7] G. KOCSIS, T. BAROSS et al., "Overview Video Diagnostics for the W7-X Stellarator", *Fusion Engineering and Design*, **96-97**, 808-811 (2015).
- [8] T. SZABOLICS, G. CSEH et al., "Event Detection Intelligent Camera: Demonstration of Flexible, Real-time Data Taking and Processing", *Fusion Engineering and Design*, **96-97**, 980-984 (2015).
- [9] T. SZABOLICS, G. CSEH et al., "Software Development for the Simultaneous Control of Ten Intelligent Overview Video Cameras at W7-X", Proceedings of 29th Symposium on Fusion Technology, Prague, Czech Republic, September 5-9, 2016.
- [10] S. ZOLETNIK, T. SZABOLICS et al., "EDICAM (Event Detection Intelligent Camera)", *Fusion Engineering and Design*, **88**, 1405-1408 (2013).
- [11] V. MARTIN, V. MONCADA et al., "Integrated Software for Imaging Data Analysis Applied

- to Edge Plasma Physic and Operational Safety”, *Fusion Engineering and Design*, **86**, 270-280 (2011).
- [12] V. MARTIN, J.M. TRAVERE et al., ”Thermal Event Recognition Applied to Protection of Tokamak Plasma-Facing Components”, *IEEE Transactions on Instrumentation and Measurement*, **59**, 5, 1182-1191 (2010).
- [13] A. ALI, M. JAKUBOWSKI et al., ”Experimental Results of Real-Time Protection System for Plasma Facing Components in Wendelstein 7-X at GLADIS”, *Physica Scripta* (to be published).
- [14] Z. ZHANG, ”A Flexible New Technique for Camera Calibration”, *IEEE Transactions on Pattern Analysis and Machine Intelligence*, **22**, 11, 13301334 (2000).
- [15] A. RODATOS, H. GREUNER et al., ”Detecting Divertor Damage During Steady State Operation of Wendelstein 7-X from Thermographic Measurements”, *Review of Scientific Instruments*, **87**, 2, 023506 (2016).